Ammonia synthesis over γ-Al_2O_3 pellets in a packed-bed dielectric barrier discharge reactor

Xinbo Zhu[1,*], Xueli Hu[1], Xiqiang Wu[1], Yuxiang Cai[2], Hongbin Zhang[1], Xin Tu[2,*]

[1] Faculty of Maritime and Transportation, Ningbo University, Ningbo 315211, P.R. China

[2] Department of Electrical Engineering and Electronics, University of Liverpool, Liverpool L69 3GJ, UK

Abstract

In this work, ammonia (NH_3) synthesis from N_2 and H_2 was carried out in a packed-bed dielectric barrier discharge (DBD) reactor, while three kinds of commercial packing materials including acidic γ-Al_2O_3, alkaline γ-Al_2O_3 and neutral alumina pellets were employed. The effect of packing materials on plasma-induced NH_3 synthesis was investigated and compared with an unpacked DBD reactor. The results show that the presence of packing materials enhanced the plasma-induced NH_3 synthesis by 15.6% to 44.4% compared to the plasma reaction without a packing. The highest NH_3 concentration of 1565.5 ppm was obtained over the alkaline γ-Al_2O_3 packed plasma reactor. The improvement of packing materials on plasma-induced NH_3 synthesis followed the order of alkaline γ-Al_2O_3> neutral γ-Al_2O_3 > acidic γ-Al_2O_3 > blank tube only. A series of characterizations were performed to illustrate the structure-performance relationships between plasma-induced NH_3 synthesis process and packing materials. The results showed that the basicity of the packing materials played an important role of the plasma-induced NH_3 synthesis process. The reaction mechanisms of NH_3 synthesis in the packed-bed DBD reactor were also discussed.

Keywords: Ammonia synthesis; Dielectric barrier discharge; Packed bed reactor; Plasma-catalysis; γ-Al_2O_3

1. Introduction

Ammonia (NH_3) is the world's second largest chemical product and is a crucial raw

material in fertilizer and chemical industries. Ammonia could also provide sufficient guarantee for ammonia as a power source and hydrogen storage, due to its high hydrogen content of 17.6% [1, 2]. Moreover, ammonia has the characteristics of high energy density, convenient storage and transportation, appropriate calorific value and high octane-value when using as fuel [3-5]. Therefore, ammonia is regarded as an ideal clean and sustainable energy source as the raw materials used for ammonia synthesis are renewable and abundant [6].

Conventional industrial-scale Haber-Bosch (HB) process produces NH_3 via a strict chemical process which need to create a sustained high pressure (20-40 MPa) and temperature (400-600 °C) environment which limit its applications in medium and small scales. Moreover, the severe working conditions make this method great energy consuming (1-2% of world's primary energy supply) and high CO_2 emission (roughly 300 million tons each year) [7]. With increasing population growth, the application of HB methods would correspondingly increase the energy consuming and CO_2 emission, making it more environmentally and economically unfavorable. Great efforts have been devoted for HB method improvement in the last 100 years to discover greener and more economical friendly sustainable alternatives to the HB process, including biochemical processes, electrochemical processes and non-thermal plasma (NTP) based processes [8-10]. Among these methods, plasma-based methods are particularly promising due to its characteristics of quick start, compact system and the flexibility to combine with renewable energy sources to reduce operational cost.

In general, NTP could generate highly chemically reactive species (e.g., high energy electrons, radicals, excited atoms and ions, etc.). These species could collide with reactants and even enable thermodynamically unfavorable reactions to proceed even at room temperature [11]. The aforementioned electrons and reactive species play important roles to initiate and propagate the complex physicochemical reaction matrix in NTP at near room temperature. The combination of plasma and heterogeneous catalysis (also known as “plasma-catalysis”) appeared to be promising to enhance the reaction performances including NH_3 synthesis, volatile organic compounds (VOCs) oxidation, CH_4 activation and water-gas shift reactions [12-15]. The underlying mechanisms of plasma-catalysis have been preliminarily studied and

ascribed to the interactions between plasma and catalysts. For instance, the electric field could be signified by the packing materials and result in generating of more reactive species. These species could be transported to the catalyst layer and participate the surface reactions. Moreover, the physical properties of the catalysts may also be modified by exposure to a plasma [16, 17].

Recently, plasma-catalytic synthesis of NH_3 has drawn attention. An early study reported NH_3 synthesis in a N_2-H_2 mixture in a strong electric field at ambient pressure. The NH_3 yield of 0.5% (v/v) was observed when MgO powder was used as a catalyst, which was more than 50% higher than that of using plasma alone [18]. Mizushima et al. investigated NH_3 synthesis in a DBD reactor with a tubular membrane-like alumina tube as a catalyst. The presence of a series of metal element (Ru, Pt, Ni, and Fe) as the catalytic active phase significantly improved the outlet NH_3 yield by 40 to 100%, while the highest NH_3 concentration was achieved when using Ru as the active phase of catalyst at the voltage of 4.5kV and flow rate of 30 $mL \cdot min^{-1}$ [19, 20]. Gómez-Ramírez et al. employed a ferroelectric packed-bed reactor for NH_3 synthesis from N_2 and H_2 under plasma treatment. Compared with $BaTiO_3$, PZT showed better energy efficiency (max. 0.9 $g \cdot kWh^{-1}$) and higher N_2 conversion rate (2.7%), respectively, indicating that the ferroelectric materials play both catalytic and electric roles in the plasma-induced reactions [21, 22]. More recently, Wang et al. studied the effect of transition metal on plasma-enhanced catalytic synthesis of NH_3 directly from N_2 and H_2 at near room temperature (~35 °C) and ambient pressure with a specially designed water-electrode equipped DBD reactor, while the Ni/Al_2O_3 catalyst showed the highest NH_3 synthesis rate among the tested samples [13].

Most of these studies investigated the effect of catalyst compositions (especially the active phase) and reaction conditions on the NH_3 performance in plasma-catalysis system, while the effects of surface characteristics of the packing materials on NH_3 synthesis were far from clearly understood . In this work, NH_3 synthesis from N_2 and H_2 in a co-axial DBD reactor was investigated over three different packing materials including acidic γ-Al_2O_3, alkaline γ-Al_2O_3 and neutral γ-Al_2O_3. The effects of working conditions, packing materials on NH_3 concentration and energy efficiency was analyzed and compared with the case of using plasma alone. A series of material characterizations were performed to illustrate the structure-

performance relationships between the packing material and NH_3 synthesis. The NH_3 synthesis reaction mechanisms were discussed and the reaction performance of plasma-catalytic synthesis of NH_3 in this work was compared with the literature.

2. Experimental section

2.1 Experiment setup

Figure 1 shows the schematic diagram of the experimental setup. For all experiments, the reactant gases (N_2 and H_2) were pre-mixed before being introduced to the DBD reactor. The two gas flows were controlled by mass flow controllers (Sevenstars, DB-07, China). Total flow rate of all experiments was fixed at 100 mL·min^{-1} unless otherwise specified. The reactor was powered by an AC discharge power source (Suman, CTP-2000K, China). The generated NH_3 was measured using a gas analyzer (Gasmet Dx4000, Finland) with the accuracy of ±3%. During the experiments, the DBD reactor was fan-cooled during the experiments. The temperature of the outer wall of the DBD reactor was around 90-105°C by an infrared thermometer (Omega, OS530, USA).

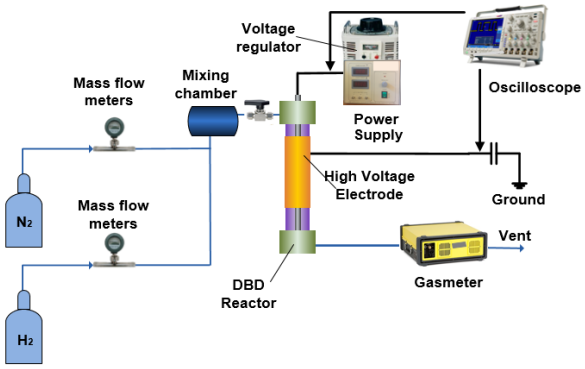

Figure 1. The schematic diagram of the experimental setup.

The DBD reactor was a concentric cylinder. A cylindrical quartz tube with an inner diameter of 8 mm and wall thickness of 1 mm was used as a discharge barrier. The quartz tube was wrapped by a 60 mm-long alumina mesh. The alumina mesh acted as a ground electrode in this work. A stainless-steel rod (4 mm in diameter) was placed on the axis of the quartz tube and connected to the AC power supply as the high voltage electrode, which resulted in the width of discharge gap of 2 mm. The discharge was limited in the space between the stainless-

steel rod and the inner surface of quartz tube. The packing materials (40-60 meshes) were randomly packed and held by glass wool in the reactor. All packing materials were of analytic grade and purchased from Aladdin Co. Ltd..

All the experiments were carried out at ambient pressure. The DBD reactor was energized when both N_2 and H_2 gas flows reached a steady state. The discharge power was measured using the Q-U Lissajous method. The applied voltage across the reactor was measured with a high voltage probe (Tektronix P6015A, 1000:1, USA), while the voltage across the measuring capacitor (1 μF) was measured with a non-source voltage probe (Tektronix TPP0500, USA). All signals were monitored by a digital oscilloscope (Tektronix DPO2014, USA). The power deposited to the reactor could be calculated as:

$$P(W) = f \times C_m \times A \tag{1}$$

where C_m is the measuring capacitance, f is the AC frequency and A is the area of the Lissajous diagram.

The specific input energy (SIE) defined as energy dissipated to the gas stream per unit volume is expressed as follow:

$$SIE\left(\mathrm{kJ \cdot L^{-1}}\right) = \frac{\mathrm{P(W)}}{\mathrm{Q\left(mL \cdot min^{-1}\right)}} \times 60 \tag{2}$$

where Q denotes the total flow rate.

Energy efficiency (EE) of the plasma-induced NH_3 synthesis process is defined as follows:

$$Energy\ Efficiency\left(\mathrm{g \cdot kWh^{-1}}\right) = \frac{M \times C_{out} \times Q_{after}}{P} \tag{3}$$

where M is the molar mass of NH_3, C_{out} denotes the outlet NH_3 concentration and Q_{after} is the outlet gas flow rate after reaction.

2.2 Material characterizations

The textural properties of the γ-Al_2O_3 samples were measured using N_2 adsorption-desorption experiments at 77 K. The samples were degassed at 200 °C for 5 h before each measurement. The specific surface area (S_{BET}) of the samples were obtained using the

Brunauer–Emmett–Teller (BET) equation.

The X-ray diffraction (XRD) patterns of the samples were measured using a Rikagu D/max-2000 X-ray diffractometer. The instrument was equipped with a Cu-Kα radiation source, All samples were scanned in the range of 10° to 80° with the step size of 0.02°.

The basicity of the samples was analyzed by temperature-programmed desorption of CO_2 (CO_2-TPD). In each test, 100 mg catalyst samples were pre-treated at 250 °C in an Ar flow for 1 h to remove the weakly adsorbed impurities before being cooled down to 50 °C . The sample was then heated to 800 °C at a heating rate of 10 °C·min^{-1} in a 5 vol.% CO_2/Ar flow at the flow rate of 40 mL·min^{-1}. The CO_2 desorption amount was calculated by the integrating the CO_2-TPD profiles.

3. Results and discussions

3.1 Characterization of catalysts

The textural properties of all three γ-Al_2O_3 samples were obtained using N_2 adsorption-desorption experiment (in **Table 1)**. All three γ-Al_2O_3 samples show similar physical properties in specific surface area (~152 $m^2 \cdot g^{-1}$), total pore volumes (~0.26 $cm^3 \cdot g^{-1}$) and average pore size (centered around 6.7 nm). The XRD patterns of all three samples are given in **Figure 2**. It is obvious that all three patterns show typical diffraction peaks of γ-Al_2O_3 centered at 37.6°, 45.9°and 67.0°, corresponding to the cubic structure of γ-Al_2O_3 crystalline (JCPDS 00-010-0425). No identical diffraction peaks of species other than γ-Al_2O_3 are detected, indicating all three samples possess the same crystal structures.

Table 1. Physico-chemical properties of the γ-Al_2O_3 samples.

Catalyst	S_{BET} ($m^2 \cdot g^{-1}$)	Total pore volume ($cm^3 \cdot g^{-1}$)	Average pore size (nm)	Amount of CO_2 desorption (mmol·g^{-1})
Acidic γ-Al_2O_3	152	0.25	6.7	0.60
Alkaline γ-Al_2O_3	154	0.27	6.8	1.13
Neutral γ-Al_2O_3	152	0.26	6.7	0.94

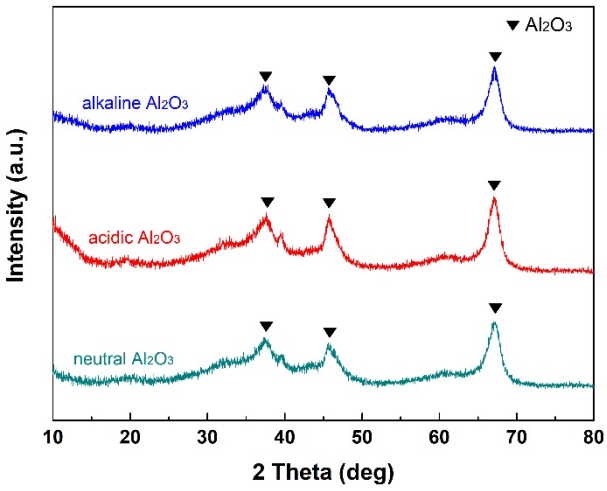

Figure 2. XRD patterns of the γ-Al_2O_3 samples.

The basicity of all three samples were measured using CO_2-TPD experiment and the profiles are presented in **Figure 3**. All CO_2-TPD profiles of the γ-Al_2O_3 show two distinct CO_2 desorption peaks. The peaks located between 100-200°C could be ascribed to the weak basic sites on the surfaces of γ-Al_2O_3, while the peaks centered at 350–450°C belong to the strong basic sites [23, 24]. The CO_2 desorption amount of all three γ-Al_2O_3 is calculated based on the CO_2-TPD profiles (in **Table 1**). It can be seen that the highest CO_2 desorption amount of 1.13 $mmol \cdot g^{-1}$ is observed over alkaline γ-Al_2O_3. The desorption amount of all three γ-Al_2O_3 follow the order of alkaline γ-Al_2O_3 > neutral Al_2O_3 > acidic γ-Al_2O_3, indicating the highest basicity of alkaline γ-Al_2O_3 in this work.

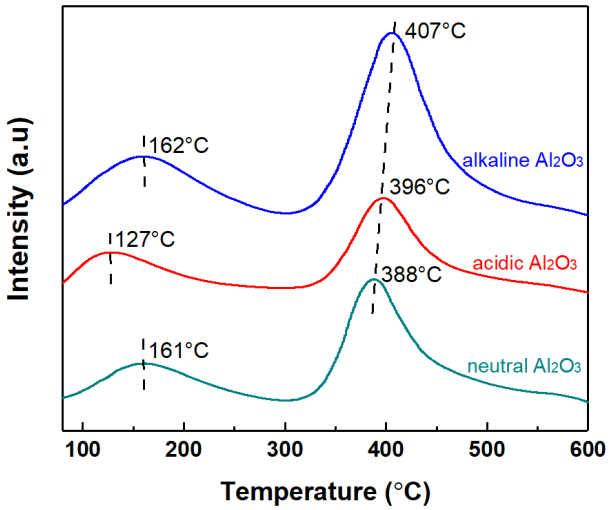

Figure 3. CO_2-TPD profiles of the γ-Al_2O_3 samples.

3.2 Effect of feeding gas ratio and flow rate

Figure 4 shows the effect of feeding gas ratio on plasma-catalytic synthesis of NH_3 over the γ-Al_2O_3 packed and non-packed DBD reactor at different N_2/H_2 molar ratios (1:5, 1:3, 1:1, 3:1 and 5:1) at the SIE of 12.0 $kJ \cdot L^{-1}$. Compared with the non-packed reactor, the presence of packing materials improved the NH_3 concentration over the tested N_2/H_2 molar ratios. It is interesting to note that for all packing materials, the highest NH_3 concentration is obtained at the molar ratio of 1:1 instead of the stoichiometric N_2/H_2 molar ratio of 1:3. Previous studies reported that the dissociation of triple bond in N_2 molecules is the rate determining step in NH_3 synthesis due to the higher dissociation energy of N_2 (9.8 eV) compared to that of H_2 (4.5 eV) [13]. Thus, it could be deduced that increasing of N_2/H_2 may increase the possibilities of effective collisions between high energy electrons and N_2 molecules, which lead to the dissociation of N_2 molecules and generate more N· radicals in the plasma regions especially in N_2-rich conditions [25]. Consequently, the NH_3 concentration was increased. Similar optimum N_2/H_2 ratios were reported in Xie et al. and Peng et al.'s work [26, 27].

Figure 5 presents the effect of gas flow rate on plasma-catalytic synthesis of NH_3 at the SIE of 12.0 $kJ \cdot L^{-1}$. The NH_3 concentration follows the order of alkaline γ-Al_2O_3 > neutral Al_2O_3 > acidic γ-Al_2O_3 > blank tube reactor. The highest NH_3 concentration of 2079.1 ppm is obtained at the minimum gas flow rate of 50 $mL \cdot min^{-1}$ over alkaline γ-Al_2O_3. Further increasing the gas flow rate decreases the NH_3 concentration. Similar results were widely reported for plasma-catalytic reactions as the residence time of gas mixtures were prolonged at lower gas flow rate. For a given reactor configuration and constant reaction conditions, the number density and electron energy distribution function (EEDF) of generated energetic electrons and reactive species were the same [28]. Thus, with longer residence time, the possibilities of effective collisions between the electrons and reactive species were enhanced no matter on the surfaces of packing materials or in the gas phase, leading to an improvement in the generation of more NH_3 in the reactor. A similar phenomenon was also reported in the plasma processing of N_2 and H_2 using a non-packed DBD reactor [26].

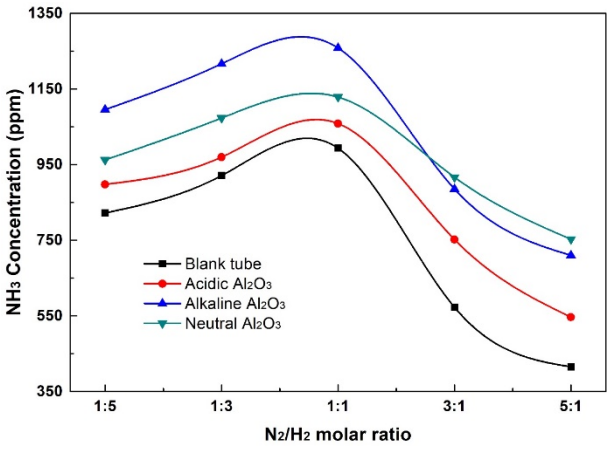

Figure 4. Effect of N_2/H_2 molar ratio on plasma-catalytic synthesis of NH_3 over γ-Al_2O_3 in terms of outlet NH_3 concentration (Reaction conditions: SIE=12 kJ·L^{-1}, N_2/H_2 molar ratio=1:3).

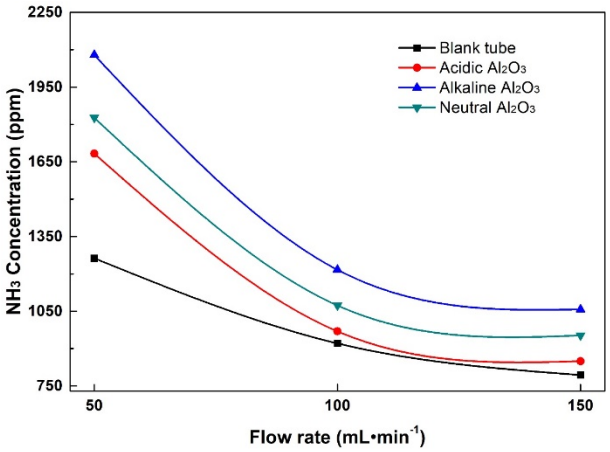

Figure 5. Effect of total flow rate on plasma-catalytic synthesis of NH_3 over γ-Al_2O_3 in terms of outlet NH_3 concentration (Reaction conditions: SIE=12 kJ·L^{-1}, N_2/H_2 molar ratio=1:3).

3.3 Effect of specific input energy (SIE)

Figure 6 presents the effect of different packing material on the performance of plasma-catalytic synthesis of NH_3 in terms of NH_3 concentration and energy efficiency of the process. Clearly, both NH_3 concentration and energy efficiency of the plasma-catalytic process increase with SIE regardless of the packing material used. As given in **Figure 6a**, NH_3 concentration in the blank tube case increases from 124.5 ppm to 1120.6 ppm in the SIE range of 3.71 kJ·L^{-1} to 14.52 kJ·L^{-1}. The introduction of alkaline γ-Al_2O_3 significantly improve the NH_3 concentration over the tested SIE range by 15.6% to 44.4%, while the enhancement is observed only over high SIE in presence of other two types of γ-Al_2O_3. The highest NH_3 concentration of 1565.5

ppm is obtained over packed DBD reactor at the SIE of 14.55 kJ·L^{-1}. This phenomena indicates the role of surface chemistry of the packing material, γ-Al_2O_3, for NH_3 synthesis in plasma environment. It is well recognized that increasing the SIE could effectively enhances the electric field in the plasma region and result in the generation of more highly energetic electrons [29]. As with the case of NH_3 synthesis, these species are capable to collide with the N_2 and H_2 molecules to generate N·, H· radicals and N_2^+ ions [13, 30]. The number densities of these species increased with discharge voltage as confirmed using optical emission spectra (OES), resulting in the generation of more NH· radicals by recombination, the major precursor of NH_3 formation, in the plasma-catalytic system [31]. Moreover, the reactions between free radicals and vibrational excited N_2 and H_2 molecules were recognized to be more important than ion reactions on NH_3 synthesis [32]. Similarly, the energy efficiencies of the plasma-catalytic process increase with the increased SIE for all cases, while the highest energy efficiency of 6.58 g·kWh^{-1} is achieved at the SIE of 14.55 kJ·L^{-1} over alkaline γ-Al_2O_3 (**Figure 6b**). This could be ascribed to the activation and dissociation of chemical bonds in N_2 and H_2 at higher SIE, leading to the generation of more NH_3.

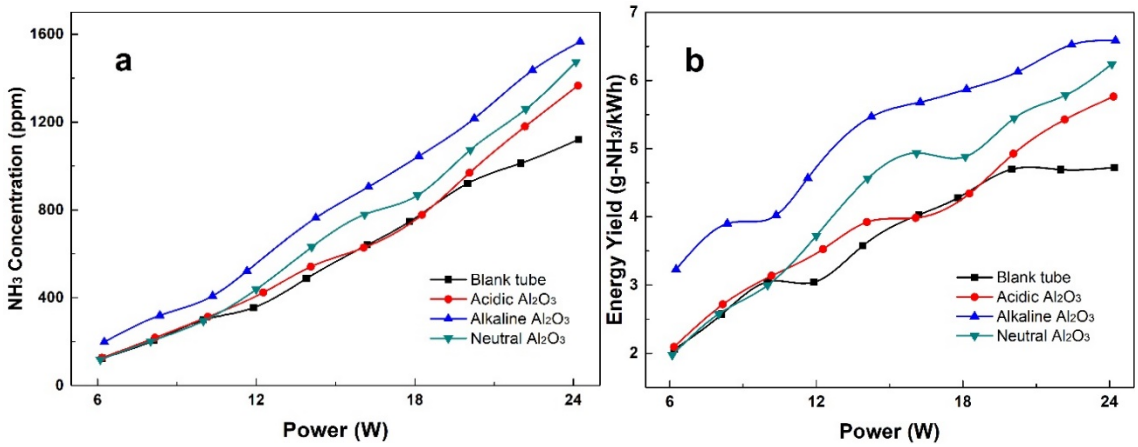

Figure 6. Effect of SIE on plasma-catalytic synthesis of NH_3 over γ-Al_2O_3: (**a**) outlet NH_3 concentration, (**b**) energy efficiency of the process (Reaction conditions: N_2/H_2 molar ratio = 1:3; Q=100mL·min^{-1}).

In this study, it is clear that the performance of plasma-catalytic NH_3 synthesis mainly depends on the properties of the packing materials. As the physical properties of the packing materials were almost the same, it can be deduced that the chemical properties on the γ-Al_2O_3

may play a more important role. Previous works also evidenced that in single-stage plasma-catalytic system, plasma-induced surface reactions played a crucial role as the packing materials were directly in contact with plasma discharge besides the reactions in gas phase. In plasma region, the generated reactive N· and H· species could also be transported and adsorbed on the surface of the packed γ-Al_2O_3 together with NH_x· (x=1, 2) radicals [33]. The metastable species like N_2(A) may contribute to the adsorption of radicals and accelerate the surface reactions. The N_2 adsorption-desorption and XRD results showed that the packed γ-Al_2O_3 possessed similar physical properties. It could be deduced that the enhancement of electric field in the packed-bed DBD reactors were almost the same considering the powder sizes and the physical properties [28]. As given in **Figure 3**, all CO_2-TPD profiles of the γ-Al_2O_3 samples shows two major CO_2 desorption peaks, and the desorption peaks belong to strong basic sites are much larger than that of weak basic sites. The amount of CO_2 desorption and maximum desorption temperature of CO_2 could be used to determine the amount and strength of basic sites respectively [24]. Moreover, the basicity of the packed γ-Al_2O_3 follows the order of alkaline γ-Al_2O_3 > neutral Al_2O_3 > acidic γ-Al_2O_3. It was well recognized that the activity of NH_3 synthesis was closely correlated to the basicity of the catalyst due to the electron-donating effect of the basic sites [23]. The surfaces with more strong basics sites tended to offer an electron-rich environment in plasma-catalytic synthesis of NH_3, and consequently contribute to the enhancement of N_2 dissociation of the γ-Al_2O_3 in this work. Considering the synergistic effect in the plasma-catalytic synthesis of NH_3 occurred between both gas phase and solid phase [11]. Thus, the adsorbed N·and NH_x (x=1, 2) may follow a stepwise hydrogenation reactions with H· in gas phase and on catalyst surfaces, forming NH_3 molecules in the plasma-catalytic system under both the Eley-Rideal (E-R) mechanisms and the Langmuir-Hinshelwood (L-H) mechanisms [13]. Based on the discussions, the reaction mechanisms of plasma-catalytic NH_3 synthesis over γ-Al_2O_3 were presented in **Figure 7**.

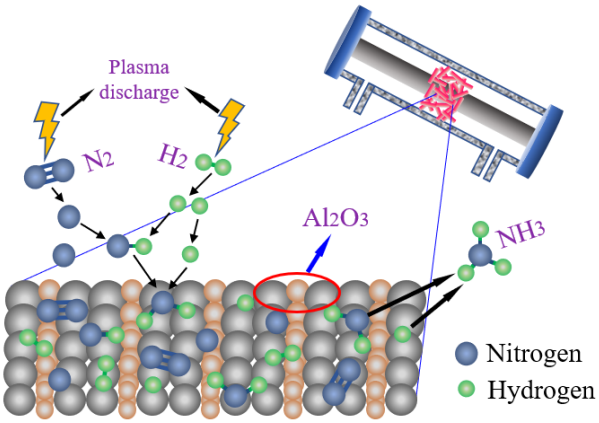

Figure 7. Reaction mechanisms of plasma-catalytic NH_3 synthesis over γ-Al_2O_3.

3.4 Comparisons of reaction performance with literature

Figure 8 compares the performance of plasma-catalytic synthesis of NH_3 in terms of NH_3 concentration and energy efficiency of the process, while the data is derived from the literature. It can be seen that the NH_3 concentration and energy efficiency of the plasma-catalytic process increases simultaneously with the increasing SIE under the given working conditions and fixed plasma reactor configuration. This could be ascribed to the generation of more chemically reactive radicals from N_2 and H_2 in the plasma-catalytic systems, while all the generated species could contribute to the formation of NH_x (x=1,2), the major precursors of NH_3, with no energy was used to ionize the carrier gas molecules that didn't participate in the final product (unlike the case of waste gas treatment) [34].

It could be summarized that the energy efficiency and total energy consumption at a certain outlet NH_3 concentration majorly depended on the reactor configuration and working conditions. For example, Xie et al. investigated the one-step synthesis of NH_3 in an Al_2O_3 packed DBD reactor. The NH_3 concentration of 46.3 ppm and energy efficiency of 0.62 $g \cdot kWh^{-1}$ was achieved simultaneously at the SIE of 8.4 $kJ \cdot L^{-1}$ [35]. As with Ruan et al.'s work, a NH_3 outlet concentration of 45 ppm and energy efficiency of 1.70 $g \cdot kWh^{-1}$ were obtained at a high SIE of 124 $kJ \cdot L^{-1}$ over a Ru/Si-MCM-41 catalyst [36]. Murphy et al. reported a NH_3 synthesis in a diamond-like-carbon coated α-Al_2O_3 spheres packed DBD reactor. The outlet NH_3 concentration of 3150 ppm and energy efficiency of 0.18 $g \cdot kWh^{-1}$ were obtained at the SIE of 43.4 $kJ \cdot L^{-1}$ [37]. In this work, a relative high energy efficiency was achieved at low SIE,

indicating the potential of alkaline γ-Al_2O_3 as a catalyst for plasma-catalytic process. However, the concentration of outlet NH_3 was not high enough. Therefore, the balance between total energy consumption and reaction performance in terms of NH_3 concentration and energy efficiency should be considered and optimized for further development and optimization of a cost-effective plasma-catalytic process for NH_3 synthesis on a wide range of plasma operating conditions.

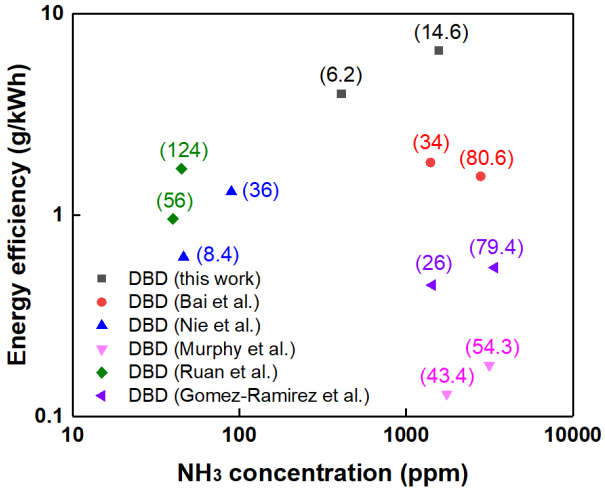

Figure 8. Comparison of NH_3 concentration and energy efficiency of plasma-catalytic synthesis of NH_3 with previous studies (The numerals in the brackets are the corresponding SIE of the presented energy efficiency in the literature, unit: $kJ \cdot L^{-1}$).

4. Conclusions

NH_3 synthesis from N_2/H_2 mixtures was carried out at ambient pressure in a packed-bed DBD reactor, while three kinds of commercial packing materials include acidic γ-Al_2O_3, alkaline γ-Al_2O_3 and neutral alumina pellets were employed. The outlet NH_3 concentration increased with increasing SIE of the DBD reactor. The presence of all types of γ-Al_2O_3 enhanced the plasma-catalytic synthesis of NH_3 compared with the unpacked DBD reactor by 15.6% to 44.4%. The highest NH_3 concentration of 1565.5 ppm was obtained over the alkaline γ-Al_2O_3 packed plasma reactor at the SIE of 14.55 $kJ \cdot L^{-1}$. The enhancement of packed material on plasma-induced NH_3 synthesis followed the order of alkaline γ-Al_2O_3 > neutral γ-Al_2O_3 > acidic γ-Al_2O_3. The highest energy efficiency of 6.58 $g \cdot kWh^{-1}$ was also obtained at the SIE of

14.55 $kJ \cdot L^{-1}$ over alkaline γ-Al_2O_3. The effects of N_2/H_2 molar ratio and gas flow rate on plasma-catalytic NH_3 synthesis were also studied. The optimum N_2/H_2 molar ratio in this work was 1:1, indicating the N_2-rich environment was favorable for NH_3 synthesis due to the generation of more N radicals under the treatment of plasma, while higher gas flow rate reduced the outlet NH_3 concentration. A series of characterizations including N_2 adsorption-desorption, XRD and CO_2-TPD were performed to illustrate the structure-performance relationships between plasma-induced NH_3 synthesis process and the packing materials. Since the physical properties of all three γ-Al_2O_3 are almost the same. The enhancement in reaction performance was attributed to basicity of the packing materials due to the electron-donating effect of basic sites on catalyst surfaces, as the order of enhancement effect were in consistent with that of basicity. The reaction mechanisms of NH_3 synthesis in γ-Al_2O_3 packed-bed DBD reactor were proposed.

Acknowledgements

The authors are grateful for the financial support from National Natural Science Foundation of China (No.51976093), Natural Science Foundation of Ningbo (2018A610207) and K.C. Wong Magna Fund in Ningbo University.

References

[1] Kim H H, Teramoto Y, Ogata A, Takagi H and Nanba T 2017 Atmospheric-pressure nonthermal plasma synthesis of ammonia over ruthenium catalysts *Plasma Process. Polym.* **14** 1600157

[2] Zamfirescu C and Dincer I 2008 Using ammonia as a sustainable fuel *J. Power Source.* **185** 459-65

[3] Wang W, Herreros J M, Tsolakis A and York A P E 2013 Ammonia as hydrogen carrier for transportation; investigation of the ammonia exhaust gas fuel reforming *Int. J. Hydrogen Energ.* **38** 9907-17

[4] Klerke A, Christensen C H, Nørskov J K and Vegge T 2008 Ammonia for hydrogen storage: challenges and opportunities *J. Mater. Chem.* **18** 2304

[5] Zamfirescu C and Dincer I 2009 Ammonia as a green fuel and hydrogen source for vehicular applications *Fuel Process. Technol.* **90** 729-37

[6] Muradov N and Vezirolu T 2005 From hydrocarbon to hydrogen? Carbon to hydrogen economy *Int. J. Hydrogen Energ.* **30** 225-37

[7] Erisman J W, Sutton M A, Galloway J, Klimont Z and Winiwarter W 2008 How a century of ammonia synthesis changed the world *Nat. Geosci.* **1** 636-39
[8] Montoya J H, Tsai C, Vojvodic A and Norskov J K 2015 The challenge of electrochemical ammonia synthesis: A New perspective on the role of nitrogen scaling relations *ChemSusChem* **8** 2180-6
[9] Eschenlauer S C, McKain N, Walker N D, McEwan N R, Newbold C J and Wallace R J 2002 Ammonia production by ruminal microorganisms and enumeration, isolation, and characterization of bacteria capable of growth on peptides and amino acids from the sheep rumen *Appl. Environ. Microbiology* **68** 4925-31
[10] Patil B S, Wang Q, Hessel V and Lang J 2015 Plasma N_2-fixation: 1900-2014 *Catalysis Today* **256** 49-66
[11] Whitehead J C 2016 Plasma-catalysis: the known knowns, the known unknowns and the unknown unknowns *J. Phys. D: Appl. Phys.* **49** 243001
[12] Kim J, Go D B and Hicks J C 2017 Synergistic effects of plasma-catalyst interactions for CH4 activation *Phys. Chem. Chem. Phys.* **19** 13010-21
[13] Wang Y, Craven M, Yu X, Ding J, Bryant P, Huang J and Tu X 2019 Plasma-enhanced catalytic synthesis of ammonia over a Ni/Al_2O_3 catalyst at near-room temperature: Insights into the importance of the catalyst surface on the reaction mechanism *ACS Catalysis* **9** 10780-93
[14] Zhang Z, Jiang Z and Shangguan W 2016 Low-temperature catalysis for VOCs removal in technology and application: A state-of-the-art review *Catal. Today* **264** 270-78
[15] Xu S, Chansai S, Stere C, Inceesungvorn B, Goguet A, Wangkawong K, Taylor S F R, Al-Janabi N, Hardacre C, Martin P A and Fan X 2019 Sustaining metal–organic frameworks for water–gas shift catalysis by non-thermal plasma *Nat. Catal.* **2** 142-48
[16] Neyts E C 2015 Plasma-Surface Interactions in Plasma Catalysis *Plasma Chem. Plasma Process.* **36** 185-212
[17] Kim H-H, Teramoto Y, Negishi N and Ogata A 2015 A multidisciplinary approach to understand the interactions of nonthermal plasma and catalyst: A review *Catal. Today* **256** 13-22
[18] Bai M D, Bai X Y, Zhang Z T and Bai M D 2000 Synthesis of ammonia in a strong electric field discharge at ambient pressure *Plasma Chem. Plasma Process.* **20** 511-20
[19] Mizushima T, Matsumoto K, Ohkita H and Kakuta N 2007 Catalytic effects of metal-loaded membrane-like alumina tubes on ammonia synthesis in atmospheric pressure plasma by dielectric barrier discharge *Plasma Chemistry and Plasma Processing* **27** 1-11
[20] Mizushima T, Matsumoto K, Sugoh J, Ohkita H and Kakuta N 2004 Tubular membrane-like catalyst for reactor with dielectric-barrier-discharge plasma and its performance in ammonia synthesis *Appl Catal A: Gen.* **265** 53-59
[21] Gómez-Ramírez A, Cotrino J, Lambert R M and González-Elipe A R 2015 Efficient synthesis of ammonia from N_2 and H_2 alone in a ferroelectric packed-bed DBD reactor *Plasma Source Sci. Technol.* **24** 065011

[22] Gómez-Ramírez A, Montoro-Damas A M, Cotrino J, Lambert R M and González-Elipe A R 2016 About the enhancement of chemical yield during the atmospheric plasma synthesis of ammonia in a ferroelectric packed bed reactor *Plasma Process. Polym.* **14** 1600081

[23] Narasimharao K, Seetharamulu P, Rama Rao K S and Basahel S N 2016 Carbon covered Mg–Al hydrotalcite supported nanosized Ru catalysts for ammonia synthesis *J. Mol. Catal. A: Chem.* **411** 157-66

[24] Wang Z Q, Lin J X, Wang R and Wei K M 2013 Ammonia synthesis over ruthenium catalyst supported on perovskite type $BaTiO_3$ *Catal. Comm.* **32** 11-14

[25] Jõgi I, Levoll E and Raud J 2016 Plasma oxidation of NO in O_2:N_2 mixtures: The importance of back-reaction *Chem. Eng. J.* **301** 149-57

[26] Peng P, Li Y, Cheng Y, Deng S, Chen P and Ruan R 2016 Atmospheric Pressure Ammonia Synthesis Using Non-thermal Plasma Assisted Catalysis *Plasma Chemistry and Plasma Processing* **36** 1201-10

[27] Xie D, Sun Y, Zhu T, Fan X, Hong X and Yang W 2016 Ammonia synthesis and by-product formation from H_2O, H_2 and N_2 by dielectric barrier discharge combined with an Ru/Al_2O_3 catalyst *RSC Adv.* **6** 105338-46

[28] Gallon H J, Kim H H, Tu X and Whitehead J C 2011 Microscope-ICCD imaging of an atmospheric pressure CH_4 and CO_2 dielectric barrier discharge *IEEE T. Plasma Sci.* **39** 2176-77

[29] Neyts E C, Ostrikov K K, Sunkara M K and Bogaerts A 2015 Plasma catalysis: Synergistic effects at the nanoscale *Chem. Rev.* **115** 13408-46

[30] Bai M, Zhang Z, Bai X, Bai M and Ning W 2003 Plasma synthesis of ammonia with a microgap dielectric barrier discharge at ambient pressure *IEEE Trans. Plasma Sci.* **31** 1285-91

[31] Uyama H and Matsumoto O 1989 Synthesis of ammonia in high-frequency discharges *Plasma Chem Plasma Process* **9** 13-24

[32] Hong J, Pancheshnyi S, Tam E, Lowke J J, Prawer S and Murphy A B 2017 Kinetic modelling of NH_3 production in N_2–H_2 non-equilibrium atmospheric-pressure plasma catalysis *J. Phys. D: Appl. Phys.* **50** 154005

[33] Carrasco E, Jimenez-Redondo M, Tanarro I and Herrero V J 2011 Neutral and ion chemistry in low pressure dc plasmas of H_2/N_2 mixtures: routes for the efficient production of NH_3 and NH_4^+ *Phys. Chem. Chem. Phys.* **13** 19561-72

[34] Zheng C, Zhu X, Gao X, Liu L, Chang Q, Luo Z and Cen K 2014 Experimental study of acetone removal by packed-bed dielectric barrier discharge reactor *J. Ind. Eng. Chem.* **20** 2761-68

[35] Xie Q, Zhuge S, Song X, Lu M, Ruan R, Nie Y and Ji J 2018 Hydrogenation of plasma-excited nitrogen over an alumina catalyst for ammonia synthesis *Int. J. Hydrogen Energ.* **43** 14885-91

[36] Peng P, Cheng Y, Hatzenbeller R, Addy M, Zhou N, Schiappacasse C, Chen D, Zhang Y, Anderson E, Liu Y, Chen P and Ruan R 2017 Ru-based multifunctional mesoporous catalyst for low-pressure and non-thermal plasma synthesis of

ammonia *Int. J of Hydrogen Energ.* **42** 19056-66
[37] Hong J, Aramesh M, Shimoni O, Seo D H, Yick S, Greig A, Charles C, Prawer S and Murphy A B 2016 Plasma catalytic synthesis of ammonia using functionalized-carbon coatings in an atmospheric-pressure non-equilibrium discharge *Plasma Chem. Plasma Process.* **36** 917-40